

ELECTRIC FRACTURE AND POLARIZATION SWITCHING OF PIEZOELECTRIC CERAMICS: EXPERIMENT AND FINITE ELEMENT SIMULATION

M. Karaiwa, F. Narita and Y. Shindo

Department of Materials Processing, Graduate School of Engineering, Tohoku University,
Aoba-yama 02, Sendai 980-8579, Japan

ABSTRACT

This paper presents the results of an experimental and numerical investigation in electric fracture behavior of poled PZT (lead zirconate titanate) specimens. Fracture experiments were conducted on commercial soft type piezoelectric ceramics. Fracture loads under different electric fields were obtained from the experiment. Nonlinear finite element analysis was also employed to calculate the energy release rate for the PZT specimens based on the exact (permeable) and approximate (impermeable) crack models. The effects of applied electric field and polarization switching on the energy release rate are discussed, and the model predictions are compared with the results of the experiments.

1 INTRODUCTION

PZT piezoelectric ceramics are widely used in piezoelectric devices, e.g., sensors, actuators, and transformers. In most of these applications the PZT ceramics are exposed to high mechanical stresses and intense electric fields which may result into failure or dielectric breakdown. Considerable researches have been theoretically devoted to piezoelectric fracture problems [1, 2], and experimental studies for cracks in various PZTs have been carried out [3, 4]. Shindo *et al.* [5] made IF (indentation fracture) tests on the PZTs, and employed a finite element analysis to calculate the fracture mechanics parameters such as energy release rate. Shindo *et al.* [6] also investigated theoretically and experimentally the fracture and polarization properties of PZTs under mechanical and electrical loads utilizing the MSP (modified small punch) test technique.

The main aim of this paper is to report on recent numerical and experimental developments which propose enhancement or retardation of crack propagation in PZT ceramics by applied electrical loading. The first section examines the experiments and numerical simulations associated with a commercial soft type PZT ceramic using SEPB (single-edge precracked-beam) specimens. The fracture loads under different electric fields are obtained from the SEPB tests. A nonlinear two-dimensional finite element analysis is also employed to calculate the effects of applied electric field and polarization switching on the energy release rate for the permeable and impermeable cracks. Attempts are made to compare the results of finite element analysis with experimental observations. The second section discusses the test and finite element results for DT (double torsion) specimens. The DT tests are performed on composite PZT specimens, and the fracture loads are obtained. The electromechanical response of the DT specimen is also predicted using a nonlinear three-dimensional finite element approach, and the simulation results are compared to the experimental results.

2 BASIC EQUATIONS

The governing field equations for a ferroelectric will be summarized. Equilibrium and Gauss' law are given by

$$\sigma_{ji,j} = 0 \quad (1)$$

$$D_{i,i} = 0 \quad (2)$$

where σ_{ij} and D_i are the stress and electric displacement, and a comma followed by an index denotes partial differentiation with respect to a space coordinate x_i ($i = 1, 2, 3$). We have employed Cartesian tensor notation and the summation convention for repeated tensor indices. The strain ε_{ij} and electric field E_i are

$$\varepsilon_{ij} = \frac{1}{2}(u_{j,i} + u_{i,j}) \quad (3)$$

$$E_i = -\phi_{,i} \quad (4)$$

where u_i and ϕ are the displacement and electric potential, respectively. In a ferroelectric, domain wall motion within each grain leads to changes in the remanent strain ε_{ij}^r and remanent polarization P_i^r . The total strain and electric displacement are described by

$$\varepsilon_{ij} = \varepsilon_{ij}^1 + \varepsilon_{ij}^r \quad (5)$$

$$D_i = D_i^1 + P_i^r \quad (6)$$

where the superscript 1 denotes the linear contribution to the strain and electric displacement, and the linear piezoelectric relationships are

$$\varepsilon_{ij}^1 = s_{ijkl}\sigma_{kl} + d_{kij}E_k \quad (7)$$

$$D_i^1 = d_{ikl}\sigma_{kl} + \varepsilon_{ik}E_k \quad (8)$$

In Eqs. (7) and (8), s_{ijkl} , d_{kij} and ε_{ik} are the elastic compliance, direct piezoelectric constant and dielectric permittivity, which satisfy the following symmetry relations:

$$s_{ijkl} = s_{jikl} = s_{ijlk} = s_{jilk}, \quad d_{kij} = d_{kji}, \quad \varepsilon_{ik} = \varepsilon_{ki} \quad (9)$$

σ_{ij} and D_i^1 are related to ε_{ik} and E_i by

$$\sigma_{ij} = c_{ijkl}\varepsilon_{kl}^1 - e_{kij}E_k \quad (10)$$

$$D_i^1 = e_{ikl}\varepsilon_{kl}^1 + \varepsilon_{ik}E_k \quad (11)$$

where c_{ijkl} and e_{ikl} are the elastic and piezoelectric constants, and

$$c_{ijkl} = c_{jikl} = c_{ijlk} = c_{jilk}, \quad e_{kij} = e_{kji} \quad (12)$$

The direction of a spontaneous polarization P^s of each grain can change by 180° or 90° for ferroelectric switching induced by a sufficiently large electric field opposite to the poling direction. The 90° ferroelastic domain switching is induced by a sufficiently large stress field. The criterion states that a polarization switches when the electrical and mechanical work exceeds a critical value [7]

$$\sigma_{ij}\Delta\varepsilon_{ij} + E_i\Delta P_i \geq 2P^s E_c \quad (13)$$

where $\Delta\varepsilon_{ij}$ and ΔP_i are the changes in the spontaneous strain and polarization during switching, respectively, and E_c is a coercive electric field. The constitutive equations (10) and (11) during polarization switching are

$$\sigma_{ij} = c_{ijkl}\varepsilon_{kl}^1 - e'_{kij}E_k \quad (14)$$

$$D_i^1 = e'_{ikl}\varepsilon_{kl}^1 + \epsilon_{ik}E_k \quad (15)$$

where e'_{ikl} is the value of piezoelectric constant after switching [6].

3 SINGLE-EDGE PRECRACKED PZT CERAMICS

3.1 SEPB test

The specimen of width $W=5$ mm, thickness $B=5$ mm and length $L=15$ mm, as shown in Fig. 1(a), is commercially supplied P-7 [5]. The coercive electric field E_c is 0.8 MV/m. Poling was done along the axis of the 15 mm dimension, and electrodes were coated in silver on two $5\text{ mm} \times 5\text{ mm}$ surfaces. Eleven Vickers indents were introduced, with indentation loads of 19.6 N, and the specimens were compressed until a precrack of length a was formed.

SEPB tests were then performed using a three-point flexure fixture with a $S=13$ mm major span, and 2 mm diameter loading pins. A 250 N micro-testing machine was used with a crosshead speed of $0.2\ \mu\text{m}/\text{sec}$. Loads which caused fracture were measured for each set of specimens for various electric fields. For each electric field E_0 , at least three tests were carried out and the average results reported.

3.2 2-D finite element formulation

Plane strain finite element calculations were made to determine the energy release rate for the SEPB specimens. The specimen and loading geometries are shown in Fig. 1(b). A rectangular Cartesian coordinate system x, y, z is used with the z -axis coinciding with the poling direction. A mechanical load was produced by the application of either a prescribed force P_0 at $x=0, z=0$ along the x -direction. For electrical loads, an electric potential ϕ_0 was applied at the edge $0 \leq x \leq W, z = L/2$. The edge $0 \leq x \leq W, z = -L/2$ was grounded.

The polarization switching is defined for each element in a material. Boundary loads are applied, and the electroelastic fields of each element are computed from the finite element analysis. The switching criterion of Eq. (13) is checked for every element to see if switching will occur. After all possible polarization switching has occurred, the piezoelectric constants of each element

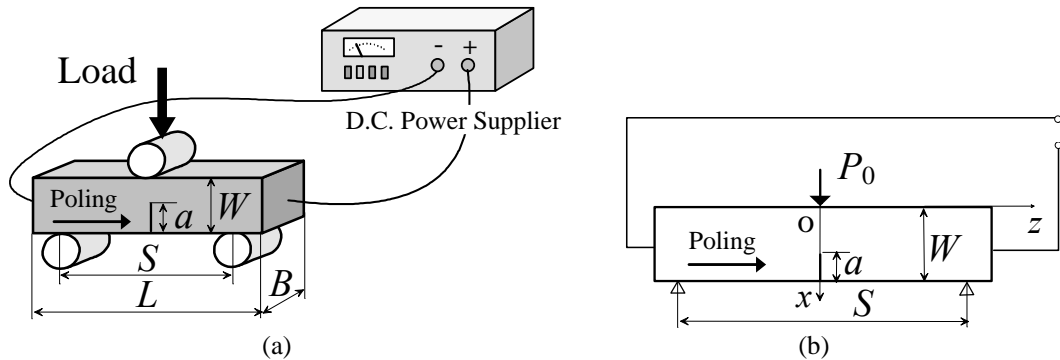


Figure 1: Schematic representation of the SEPB tests: (a) testing set-up, (b) finite element model.

are changed. The electroelastic fields are re-calculated, and the process is repeated until the solution converges. The spontaneous polarization P^s and strain γ^s are assigned representative values of 0.3 C/m^2 and 0.004 , respectively.

Due to the polarization switching, piezoelectric ceramics are often non-homogeneous. The piezoelectric properties vary from one location to the other, and the variations are either continuous or discontinuous. The energy release rate G can be obtained from the following crack-tip integral:

$$G = \int_{\Gamma_0} (H\delta_{1j} - \sigma_{ij}u_{i,1} + D_j E_1) n_j d\Gamma - \int_{\Gamma_p} (H\delta_{1j} - \sigma_{ij}u_{i,1} + D_j E_1) n_j d\Gamma \quad (16)$$

where Γ_0 is a small contour closing a crack tip, Γ_p is a path embracing that part of phase boundary which is enclosed by Γ_0 , δ_{ij} is Kronecker delta, n_j is the unit normal vector, and a local orthogonal coordinate system is employed for the crack tip such that x_1 - and x_3 - axes lie parallel and normal to the crack faces, respectively. The electrical enthalpy density is expressed as

$$H = \frac{1}{2} c_{ijkl} \varepsilon_{ij} \varepsilon_{kl} - \frac{1}{2} \varepsilon_{ij} E_i E_j - e_{ikl} \varepsilon_{kl} E_i \quad (17)$$

3.3 SEPB test results and discussion

Table 1 shows the averaged fracture loads P_c for $a/W=0.1$ under different electric fields obtained from the experiment. A positive applied electric field decreases the fracture load, and a negative one increases it. Figure 2 shows the dependence of G for the exact (permeable) crack model without and with switching effect on E_0 under $P_0 = 137 \text{ N}$ for $a/W=0.1$, normalized by values for $E_0=0 \text{ V/m}$. Also shown is the result for the approximate (impermeable) crack model without switching effect. The results show that a monotonically increasing negative E_0 causes polarization switching. After E_0 reaches about -0.2 MV/m , local polarization switching can cause a rapid decrease in G for the exact crack model.

Table 1: SEPB test results

$a/W = 0.1$	
E_0 (MV/m)	P_c (N)
- 0.2	147
0	137
+ 0.2	128

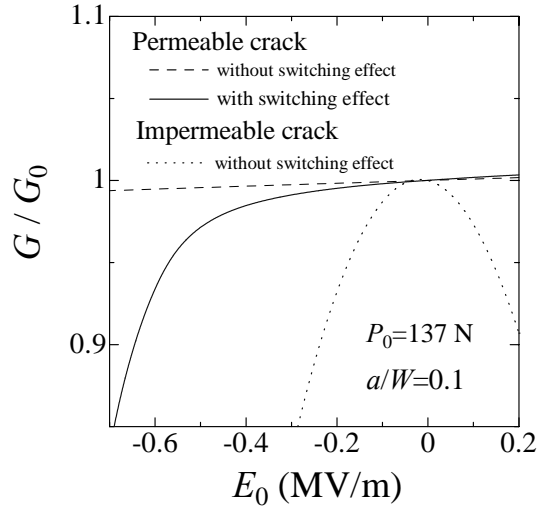


Figure 2: Energy release rate vs electric field for SEPB specimen

4 PRECRACKED DOUBLE TORSION PZT COMPOSITES

4.1 DT test

The specimen geometry used is a composite PZT DT specimen described by the Cartesian coordinate system (x,y,z) , as shown in Fig. 3. The PZT samples of width $W_p=5$ mm, thickness $d=5$ mm and length $L=30$ mm were cut. The specimen was produced by first poling a 5 mm wide PZT beam and then bonding it between two wider brass beams of $W_b=7.5$ mm, $d=5$ mm and $L=30$ mm with high strength epoxy. A side groove of depth $d-d_n=2.5$ mm and width $g_w=1$ mm was machined in the PZT. Before testing, a thin notch is cut in the end of the PZT to a depth of $d_n=2.5$ mm and a length of $a=5$ mm. The PZT was commercially supplied P-7. The Young's modulus and Poisson's ratio of brass are taken to be $E=100.6$ GPa and $\nu=0.35$.

The specimens were loaded by concentrated loads $P_0/2$ at $x=0$ mm, $y=2.5$ mm and $z=\pm 2$ mm in a screw-driven testing machine. The moment arm W_m and distance b for our loading machine were fixed at 5.5 mm and 2 mm, respectively. Fracture loads were measured for each set of specimens for various electric fields.

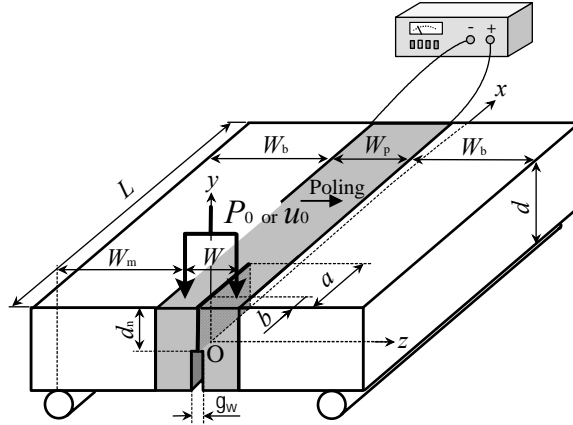


Figure 3: Schematic representation of the DT tests

4.2 3-D finite element formulation

Three-dimensional finite element calculations were made to determine the G for the composite DT specimens. A mechanical load was produced by the application of $P_0/2$ at $x=0$, $y=d_n$ and $z=\pm W/2$. For electrical loads, ϕ_0 was applied at the interface, $-b \leq x \leq L-b$, $-(d-d_n) \leq y \leq d_n$, $z=W_p/2$. The interface $-b \leq x \leq L-b$, $-(d-d_n) \leq y \leq d_n$, $z=-W_p/2$ was grounded.

4.3 DT test results and discussion

Figure 4 shows the measured fracture loads P_c for $a=5$ mm under electric fields $E_0=0, \pm 0.05, \pm 0.1$ MV/m. A positive electric field increases the fracture load, while a negative one decreases it. The numerical results for $a=5$ mm are summarized in Fig. 5 which shows the energy release rate G versus E_0 for the permeable crack model without and with switching effect under $P_0 = 205$ N, divided by G_0 for $E_0=0$ V/m. Also shown is the result for the impermeable crack model without switching effect. A monotonically increasing negative E_0 causes polarization reversal. Polarization switching in a local region leads to an unexpected decrease in G for the exact crack model.

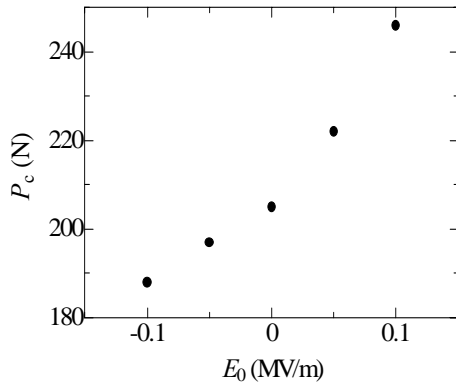


Figure 4: Fracture load vs electric field

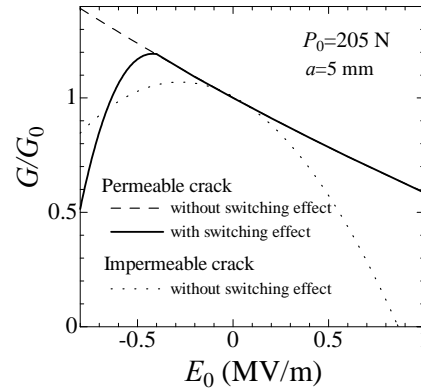


Figure 5: Energy release rate vs electric field for DT test specimens

5. CONCLUSIONS

The fracture and polarization switching behavior of piezoelectric ceramics was investigated under mechanical and electrical loads utilizing the SEPB and DT test techniques. The magnitude as well as the direction of the applied electric field is found to have a significant influence on fracture load and energy release rate. The energy release rate is also sensitive to the local polarization switching around a crack tip. The influence of electromechanical loading and polarization switching requires more research to provide deeper understanding of piezoelectric fracture for future demanding structural applications.

REFERENCES

- [1] Xu, X.-L., Rajapakse, R.K.N.D., On a plane crack in piezoelectric solids, *Int. J. Solids Structures*, 38, pp. 7643-7658, 2001.
- [2] Lin, S., Narita, F., Shindo, Y., Comparison of Energy Release Rate and Energy Density Criteria for a Piezoelectric Layered Composite with a Crack Normal to Interface, *Theoret. Appl. Fract. Mech.*, 39, pp. 229-243, 2003.
- [3] Schneider, G.A., Felten, F., McMeeking, R.M., The electrical potential difference across cracks in PZT measured by Kelvin Probe Microscopy and the implications for fracture, *Acta mater.*, 51, pp. 2235-2241, 2003.
- [4] Zhang, T.-Y., Wang, T., Zhao, M., Failure behavior and failure criterion of conductive cracks (deep notches) in thermally depoled PZT-4 ceramics, *Acta mater.*, 51, pp. 4881-4895, 2003.
- [5] Shindo, Y., Oka, M., Horiguchi, K., Analysis and testing of indentation fracture behavior of piezoelectric ceramics under an electric field, *ASME J. Eng. Mater. Tech.*, 123, pp. 293-300, 2001.
- [6] Shindo, Y., Narita, F., Horiguchi, K., Magara, Y., Yoshida, M., Electric fracture and polarization switching properties of piezoelectric ceramics PZT studies by the modified small punch test, *Acta mater.*, 51, pp. 4773-4782, 2003.
- [7] Hwang, S. C., Lynch, C. S., McMeeking, R. M., Ferroelectric/ferroelastic interactions and a polarization switching model, *Acta metall. mater.*, 43, pp. 2073- 2084, 1995.